International Journal of Engineering and Technical Research (IJETR)
ISSN: 2321-0869 (O) 2454-4698 (P), Volume-7, Issue-3, March 2017

Structural design points in arrayed micro thermal sensors (III) ~ Polymer-based approach ~

Hirofumi Miki, S. Tsuchitani

***Abstract*— In our prior work of silicon-based approach, it was understood that over 80 % of the input power that applied to the sensor was consumed at the substrate which results in the performance decrement of the sensor. To get the improved results, it is important to decrease the thermal capacity of the sensing elements and the substrate, and at the same time to improve the thermal isolation between the sensing elements and the surrounding parts (mainly the substrate and wiring) to the utmost limit. The most sensitive parameter will be the material property such as thermal conductivity. In this paper, we report the experimentally demonstrated results on the structural design points applying the fabricated prototype that based on polymer approach.**

***Index Terms*— MEMS, micro array sensor, thermal sensor, thermal isolation, fingerprint capture, structural design, polyimide film.**

I. INTRODUCTION

Silicon–based micro thermal sensors have the advantages in the arrayed micro-scale structure to measure distributed physical information like temperature or flow due to its well-established micromachining technology, and the possibility of integration with IC on the same sensor chip. However, particular attention is necessary because silicon possesses features of high thermal conductivity and mechanical brittleness. In micro thermal sensor design, the most important aspects are sensitivity, response speed, and mechanical strength. As far as the sensitivity is concerned, the contribution of the sensing-information independent heat transfer (e.g., flow-independent heat transfer in flow sensor) should preferably be small. To achieve this, the sensing area must be thermally isolated from its supporting structure sufficiently. Approach of enlarged thermal isolation cavity under the heater element will effectively improve thermal property of the sensor but greatly decrease its mechanical strength that is serious in some application like fingerprint capture. To improve thermal properties of the sensor device, one of the most sensitive parameter will be the material property such as thermal conductivity. Generally, polymer possesses the property of good thermal insulation. For example, the thermal conductivity of Kapton polyimide is even four orders of magnitude lower than that of silicon [1-4]. The combination of polymer substrate and thin metal film as the sensing element will be a cost-effective and a promising solution to realize the purpose of desirable thermal properties with simple structure. Such framework will make the device also applicable for the serious situation of fingerprint capture too. In this paper, the experimentally demonstrated results on the structural design points are reported applying the fabricated prototype that based on polymer-based approach.

Hirofumi Miki, Dept. of Systems Engineering Wakayama University 930, Sakaedani, Wakayama, Japan

S. Tsuchitani, Dept. of Systems Engineering Wakayama University 930, Sakaedani, Wakayama, Japan

II. STRUCTURE AND MATERIALS

A. Material of the sensor substrate

In the polymer-based approach, we applied a flexible polyimide (PI) film as the sensor substrate employing its splendid thermal isolation and its good balance of other material properties. PI film can retain its excellent properties of dimensional stability, thermal and electrical insulation, mechanical strength, chemical resistance, and the attractive characteristics of flexibility under a wide range of operating conditions [3-6]. In our prototype, we also used the method of vertically interconnected through-hole wiring, where micro through-holes were fabricated by PI film wet etching technology and thin metal film wiring was realized by electroless copper plating technique. Dense array of micro sensors created on a flexible PI film will be useful in MEMS applications to obtain a real-time 2- or 3-D distributed measurement of certain physical quantities such as temperature, force, and turbulent flow, as well as the application of thermal type micro fingerprint sensor. In these applications, 3-D interconnect technology is required in order to wire the dense 2-D array sensor elements easily, and make the sensing robust. Here, an important factor is to fabricate high-density micro through-holes with a low cost and high productivity. The conventional methods to fabricate micro through-holes on the PI film are by Laser, dry etching, NC drilling or punching etc. However, because of the expensive equipment, low productivity and a large amount of consuming power, the conventional fabrication methods will inevitably result in the problem of high production cost. Generally, with the methods of drilling and punching, it is also difficult to create fine through-holes and fine pitch of patterns. It is attractive to fabricate high density micro through-holes on the PI film by a wet etching technology, because, wet etching process has a significant advantage of cost effectiveness in the large-volume production. The number of holes or sizes of the hole in the same wafer does not increase the processing cost. When design a number of same holes or holes of varied sizes on the same wafer, the cost of wet etching process is significantly lower than that of conventional methods mentioned above.

In our fabrication process, we utilized PI film wet etching technology to realize the micro through-holes on the PI film. Two kinds of wet etching mask materials were used in our process, i.e. photosensitive dry film (DF) and thin copper film. 3-D interconnects metal wiring on the PI film substrate was realized by electroless copper plating technique, and the conduction of through-hole wiring was confirmed by measurement.

A-1 Molecular structures and material properties

PI film possesses a unique combination of material properties that make it ideal for a variety of applications in many different industries. Many types of PI films have been developed, but there are mainly two types in molecular structures: (1) pyromellitic acid and (2) biphenyl tetra carboxylic acid. Commercially available and the most widely used product Kapton belongs to the former, and Upilex to the latter (see Fig. 1). In MEMS structures and flexible print circuits (FPCs), the most widely used are 25~50-μm-thick flexible Kapton and Upilex PI films. In this study, we used 25-50 μm thick flexible Kapton and Upilex PI films to examine the characteristics of PI film micromachining by wet-etching technology. Kapton PI film was provided by Du Pont-Toray Co., Ltd., Japan, and Upilex PI film by UBE Industries, Ltd., Japan. Kapton, the most commonly used PI film, is synthesized by polymerizing an aromatic dianhydride and an aromatic diamine. Upilex, which has higher of the mechanical strength and thermal stability compared to Kapton, is the product of polycondensation reaction between biphenyltetracarboxylic dianhydride (BPDA) and diamine. Comparing to Kapton PI film, Upilex is relatively stronger in mechanical properties, and shows higher chemical resistance and dimensional stability over a wide range of temperature. While Kapton is stronger in folding endurance, and shows higher of the electrical resistance and lower of the thermal conductivity than Upilex PI films.

The compared results of the electrical, mechanical, thermal and chemical properties of Kapton and Upilex PI film are summarized in Table I~III and the material properties of Htype and EN-type of Kapton PI film are compared in Table IV. Both the H-type and EN-type possess PI inherent outstanding characteristics and have similar property values, but EN-type shows relatively higher dimensional stability.

A-2 Characteristics of PI film wet etching

In the PI-film wet etching process, we used a type of strong alkaline solution called TPE3000 (supplied by Toray Engineering Co., Ltd., Japan) as the etchant. TPE3000 is composed of 20wt% KOH solution and 20~40wt% aliphatic amine compound C_2H_7NO. It can hydrolyze PI and polyester compounds. When PI film is immersed in TPE3000 solution, the imide ring of the PI molecule is opened, and polymer is converted to amide that is soluble to alkaline solutions [7].

Etching rate is one of the most important parameters in the PI film micromachining. We investigated the etching rate of Kapton and Upilex PI film in TPE3000 solution by experiment, and found that it is strongly temperature dependent as shown in Fig. 2. The experimental results show that: (1) at the temperature of higher than 80°C, the etching rates increase remarkably; (2) the etching rate of the Upilex PI film is extremely lower than that of Kapton PI film. It might be derived from the strong molecular structure of Upilex which built-up its resistance to hydrolysis and inhibited itself to be etched away. At 87°C, the etching time of Upilex for per unit thickness is about 7~9 times longer than that of Kapton PI film. Along with the etching temperature rise, the etching rate differences between Kapton and Upilex PI film became larger; (3). In Kapton PI film, the etching rate of EN-type is a little higher (about 1.3 times) than that of H-type.

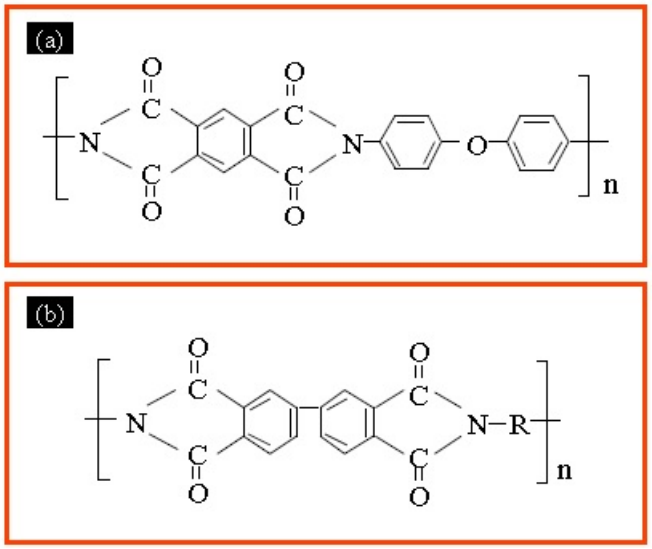

Fig. 1 PI-film molecular structures: (a) Kapton PI-film [3,5], and (b) Upilex PI-film [4,6].

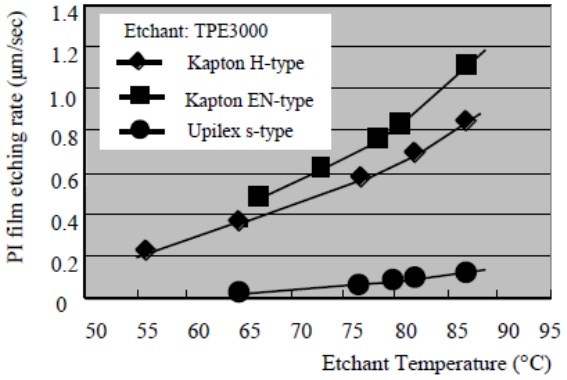

Fig. 2 PI-film wet-etching rate at the different etching temperature.

(TPE3000 solution was used as the etchant). PI film electrical properties (data from [3–6]).

Electrical properties	Kapton-100H (25 μm)	Upilex-25S (25 μm)	Test method
Dielectric strength (kV)	7.5	6.8	ASTM D149
Dielectric constant	3.4	3.5	ASTM D150
Dielectric factor	0.0018	0.0013	ASTM D150
Volume resistivity (Ω cm)	1.5×10^{17}	1.0×10^{17}	ASTM D257
Surface resistivity (Ω)	1.0×10^{16}	$>1.0 \times 10^{17}$	ASTM D257

PI FILM MECHANICAL PROPERTIES (DATA FROM [3-6])

Mechanical properties	Kapton-100H		Upilex-25S		Test method
Film thickness (μm)	25		25		
Testing temperature (°C)	23	200	25	300	
Tensile strength (MPa)	231	139	520	294	ASTM D-882
Stress at 5% elongation (MPa)	90	61	255	88	ASTM D-882
Ultimate elongation (%)	72	83	42	67	ASTM D-882
Tensile modulus (GPa)	2.5	2.0	9.121	3.727	ASTM D-882
Tear strength-initiation (graves) (N)	7.2	–	226	–	ASTM D-1004
Tear strength-propagating (elmendorf) (N)	0.07	–	3.24	–	ASTM D-1922
Folding endurance (cycles)	285 000	–	>100 000	–	ASTM D-2176
Density (g cm^{-3})	1.42	–	1.47	–	ASTM D-1505
Coefficient of kinetic friction (film-to-film)	0.48	–	0.4	–	ASTM D-1894

TABLE I. PI FILM THERMAL PROPERTIES (DATA FROM [3–6]).

Thermal properties	Kapton-100H (25 μm)	Upilex-25S (25 μm)	Test method
Melting point	None	None	ASTM E-794-85
Thermal coefficient of linear expansion (ppm °C^{-1})	20	12	ASTM D-696-91
Thermal conductivity (W/m K)	0.12	0.29	ASTM F-433-77
Specific heat (J/g K)	1.09	1.13	Differential calorimetry
Flammability	UL94-V0	UL94 VTM-0	UL-94

PI film chemical properties (data from [3–6]).

	Kapton-100H (25 μm) (%)			Upilex-25S (25 μm) (%)				
Chemical properties	Strength retained	Elongation retained	Modulus retained	Strength retained	Elongation retained	Modulus retained	Test condition	
Resistance to:								ASTM D-882
10% sodium hydroxide	–	Deteriorated	–	80	60	95	Immersion (25 °C/5 days)	
Glatial acetic acid	85	62	102	100	95	100	Immersion (110 °C/5 weeks)	
Water pH = 1.0	65	30	100	95	85	100	Immersion (100 °C/2 weeks)	
pH = 4.2				95	85	100	Immersion (100 °C/2 weeks)	
pH = 7.0	65	30	100				Immersion (100 °C/10 weeks)	
pH = 8.9				95	85	100	Immersion (100 °C/2 weeks)	
pH = 10.0	60	10	100	95	85	100	Immersion (100 °C/4 days)	
Water absorption		1.3			0.8		Equilibrium at 50% RH/23 °C	ASTM D-570
		2.9			1.4		Immersion in water 23 °C/24 h	

TABLE II. KAPTON PI FILM MAIN MATERIAL PROPERTIES (DATA FROM [3,5]).

Properties	100H	100 EN	Test method
Film thickness (μm)	25	25	
Strength (MPa)	340	350	
Elongation (%)	80	57	JIS C 2318
Young's modulus (GPa)	3.4	5.7	
Dielectric strength (kV mm^{-1})	400	390	
Heat shrinkage (%)	0.2	0.01	IPC No. 2.2.4 (200 °C)
Thermal coefficient of linear expansion (ppm °C^{-1})	27	16	50–200 °C (temperature increments (10 °C min^{-1}))
Humidity expansion Coefficient (ppm/%RH)	24	16	3–90% RH
Water absorption (%)	2.9	1.3	Immersion in water for 24 h
Thermal conductivity (W/m °C)	0.15	0.12	Model TC-1000 Comparing method
Folding endurance (cycles)	⩾20 000	⩾20 000	JIS P 8115
Volume resistivity (Ω cm)	1×10^{17}	1×10^{17}	JIS C 2318

A-3 Through-hole structure by PI film wet etching

Depending on the etching-mask material and the mask opening area, the geometry of wet-etched through-hole is different. When patterning a PI film by wet etching, the following three types of materials can be used as the etching mask: (i) a photosensitive dry film (DF), (ii) a thin Cu film (thickness > 4-μm) and (iii) a rubber-based photosensitive resist. We investigated the PI film etching characteristics in the etchant of TPE3000 solution, using photosensitive dry film and thin copper film as the etching-mask. The rubber-based photosensitive resist can also be used as the wet-etching mask, but due to the possibility of its cancerous toxic, in our experiments we excluded it from the options. In our experiments, a 15-μm thick photosensitive DF "RY-3215" was used as the wet-etching mask, which was provided by and laminated to the PI film substrate in Hitachi Chemical Co., Ltd., Japan. PI film wet etching was performed from the double sides of the substrate in TPE3000/80°C solution. The mask aperture size was Φ150-μm and the starting material was 25-μm thick EN-type Kapton PI film. The etched taper-angle θ was 44~49°. We suppose that, the fabricated etch tapers were generated by the undercut etching, and the differences of the etched taper angles were derived from the differences in the adhesiveness between the PI film and the etching-mask layer. Photosensitive DF was not as strong as the copper film and its adhesiveness to the PI film was not as strong as that of the copper film. Peeling was found in TPE3000 when the etching time was longer than 15 minutes. Based on our experiment, we recommend that when fabricate through-holes on a thicker of PI film, it is hopeful to use thin copper film as the wet-etching mask instead of DF film. However, DF mask also

has its advantage of freedom in the process design, especially, when you need to create complicate patterns with longer steps of fabrication process.

Figure 3 shows the fabricated through-hole structures by PI film wet-etching. Figure 3-a show the scanning electron microscope (SEM) images of wet-etched through-holes fabricated on the PI film using photosensitive dry film as the etching mask. The mask aperture size was Φ150-μm. Figure 3-b shows that of microscopy picture. We also fabricated through-hole structures using copper-film as the etching mask as shown in Fig. 3-c. In the copper-film-mask process, the mask aperture size was Φ50-μm and the starting material was 50-μm thick of EN-type Kapton PI film sandwiched by 5-μm thick copper film named as Metaloyal (provided by Toyo Metallizing Co., Ltd., Japan). PI film was etched in TPE3000/80°C solution from the single side of the substrate using the copper film layer as the etching-mask. Good adhesion between the etching mask and the substrate was observed during the PI wet etching, and no peeling has been found in the whole process. The thin copper film layer on the Metaloyal was formed by electrical plating technique following to an adhesion-promoting layer of 3-nm-thick sputtered chrome layer. The etched taper-angle θ was 30~35°. You can found the detailed process technology on the PI film wet etching from our prior work at ref. [8].

Below, we introduce the further information about the fabrication process of high-density micro through-holes and the 3-D interconnection-wiring with electroless copper plating technology.

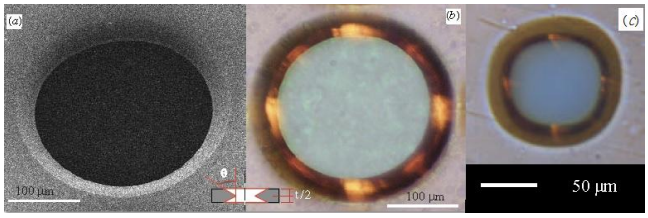

Fig. 3 Fabricated through-hole structure by PI film wet-etching: (*a*) SEM image of the sample; (*b*) That of the optical microscopy image. The starting material was 25-μm thick EN-type Kapton film. Etching mask was a laminated photo-sensitive DF RY-3215 (15-mm thick), and PI film was etched from both sides of the surfaces. (*c*) The optical microscopy image fabricated by copper-film-mask process.

A-4 3-D interconnection-wiring by electroless copper plating

In order to realize 3-D metal film interconnections on the fabricated through holes, we performed electroless copper plating process where the following solutions were used to get a well-anchored metal film:

(1) MELPLATE PC-321 (Polyoxyethylenenonylphenylether):
By dipping 50-70□ C/5min can make the inside wall of the holes on the PI film substrate in the best state for plating especially in the properties of adhesiveness;

(2) ENPLATE PC-236 (Inorganic chlorine compound): by dipping 20-35□ C/3min, can act as the pre-dipping agent for the processing catalytic agent "ENPLATE ACTIVITY 444";

(3) ENPLATE ACTIVITY 444 (Hydrogen chloride and stannous chloride): it is a catalytic agent of tin-palladium. By dipping 20-35□ C/5min, can make closely cohesive electroless copper plating to be deposited on to inside wall of the through-holes;

(4) MELPLATE PA-360 (Organic acid salt): by dipping 20-30□ C/5min, can activate the catalyzed palladium and improve the early stage deposition of electroless copper plating and make the formed metal film uniform with better of the strength. By MELPLATE CU-5100/ (45-55□ C), in about 15 minutes of time 1-μm thick copper film was created on the PI film substrate, and by MELPLATE CU-390/ (45-55□ C), as thin as 0.1-μm of copper film can be obtained. The conduction of through-hole wiring was realized and confirmed by measurement.

Generally, the adhesion of Cu to the PI film was poor, except on the area of wet-etched through-holes. Surface modification techniques such as chemical etching, plasma treatments and ultraviolet irradiation, as well as the thermal treatment, have shown to improve the adhesiveness of thin metal films to the PI film surface [9]. Chemical etching is a good choice of low cost method and can be used without extra investment. When the electroless copper plating was performed after PI film wet treatment in TPE3000 solution at 70□ C for 7 second, the adhesion of the Cu plating to the PI film can be greatly improved. The improved adhesion probably derived from the PI film wet-etching mechanism. In wet treatment, the reaction not only etches away some of the PI but also converts some into an amide that would adhere better to metals [7].

B. Material of sensing element

In our silicon-based prototype, the heater element's thermal resistance showed only slight differences in the ambient of air and vacuum. It means that most of the heat generated in the heater element was transferred to the silicon substrate. In practical use, only the heat transferred to the measuring object, for example in application of fingerprint capture, only the heat transferred to the fingertip can contribute to the detection of fingerprint patterns. Therefore, it is desirable in the structural design to thermally isolate heater elements from the substrate as can as possible. Sufficient thermal isolation could result in the minimization of unnecessary conductive heat loss, improvement of sensor sensitivity and also result in smaller of power consumption. To realize such a device, in our work, the sensing elements are made from platinum film micro heaters by sputter and lift-off technique. The sensing elements and feed-through are arranged on the different sides of the PI film substrate and connected by through-hole metal-film wiring, enables the layout of dense array sensing elements and their wiring become easier, results in more reliable and robust sensing for the sensor device. The flexible feature of the substrate make it easy to tape the device onto a non-planar curved surface enable to realize the possibility of a wider range of extensions in technical and applications as shown in Fig. 4.

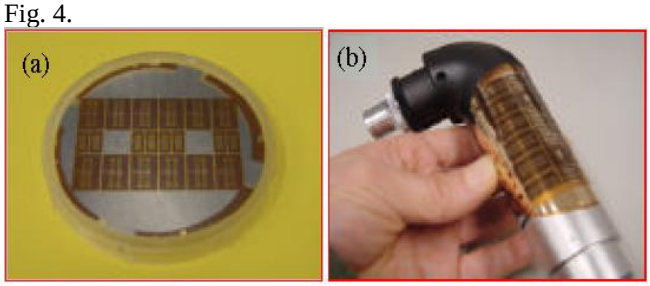

Fig. 4 The optical microscopy picture of the fabricated prototype:

(a) The whole view of the wafer size, and (b) The feature of curved prototype for the application of non-planar objects.

As described in our prior work of ref. [10], in thermal sensor the most sensitive parameter for the structure and material selection is substrate and its thermal conductivity. PI film possesses extremely low thermal conductivity (λ: 0.12 W $m^{-1}K^{-1}$ for Kapton PI film), which is three orders lower than that of silicon material (λ: 150 W $m^{-1}K^{-1}$). PI film also possesses a unique combination of properties and can retain its excellent properties of thermal and electrical insulation, mechanical strength, chemical resistance, dimensional stability and the attractive characteristics of flexibility under a wide range of operating conditions [3-6]. PI film can also be micromachined by wet etching or laser technique. Due to its unique material properties, it is a promising approach to employing the PI film as the thermal sensor substrate for the improved thermal isolation and better of sensitivity. Furthermore, because, there is no need of thermal isolation cavity, better of the mechanical strength can be obtained with simple structure. Utilizing 3-D interconnection technology, the problem of complicate overlapped wiring can be avoided in the 2-D array sensing systems where a large number of sensing elements are involved with a small pitch. Sensing elements of thin metal film can be directly deposited on the PI film substrate by vacuum deposition or sputtering. Thin metal film like copper, nickel or platinum film can be used as the low cost sensing elements. They have positive TCR with approximately linear temperature dependence. Figure 5 shows the reported results of resistance versus temperature rise on these metals. At room temperature, the coefficient $(1/R)$ (dR/dT) ranges between 3.9×10^{-3} and 6.5×10^{-3} K^{-1}. Both the copper and platinum have a TCR of near 4×10^{-3} K^{-1} and nickel.

Copper: the resistance offers the most linear temperature dependence with TCR of 4.260×10^{-3} K^{-1} for the temperatures from 0 to 100°C. Copper resistances, however, have two disadvantages that strongly limit their use: (i) at 0°C, the resistivity of copper is less than one sixth of that of platinum with about the same TCR; when the geometrical sizes of copper and platinum are same to each other, the sensitivity of a copper resistance exhibits only one sixth of platinum;
(ii) Copper begins to oxidize at the temperature above 100°C, and deteriorates rapidly at the temperature above 180°C.

Nickel: nickel has a high temperature coefficient of 6.81×10^{-3} K^{-1}. Its resistivity, however, is lower than that of platinum and the non-linearity of its resistance versus temperature characteristic is higher.

Platinum: platinum has a reasonably high temperature coefficient of 3.92×10^{-3} K^{-1} and its resistance is particularly linear with temperature [11]. Platinum resistor has a nearly constant TCR, i.e. an output that is directly proportional to temperature over a significant temperature range. More importantly, it has a high chemical stability, which enables platinum to be used as a temperature reference standard. The best stability is achieved in platinum, when the resistances made from above metals are used in air or in a mixture of helium and a small amount of oxygen [12]. Compared to other metals, platinum is relatively expensive, but, by MEMS technology the amount of platinum that is required for the sensing element is very small amount with sub-micron thickness which can make platinum a cost comparable to other materials. From Table VI, where platinum is compared to other materials, it can be concluded that, for a given resistance value, platinum always offers the possibility of smaller volume and smaller thermal mass sensors. This property has been enhanced considerably with the adoption of thin film sensors that utilize a minimum amount of platinum. When using platinum film as the sensing element and depositing to the PI film, the problem is its poor adhesion to the PI film surface. A bridge or an adhesion tie layer is required. Chromium, titanium, nickel, tantalum and palladium are often used as the tie layers. We used a 20nm-thick titanium layer as the adhesion promoter. In our process, we performed PI film surface pretreatment firstly by employing a light wet etching in a strong alkaline solution TPE3000 before sputtering titanium layer.

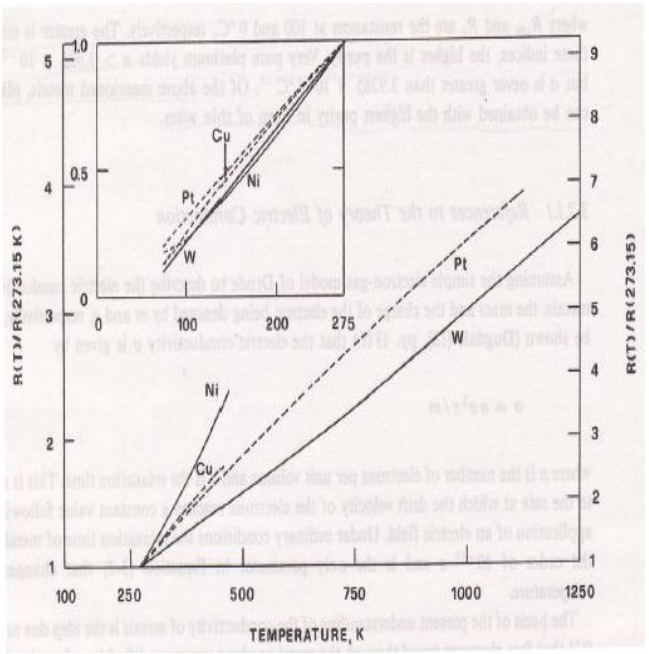

Fig. 5 Resistance of Cu, Ni, Pt, and W versus temperature rise [13].

TABLE III. MATERIAL PROPERTIES OF COPPER, NICKEL AND PLATINUM [13].

Properties \ Materials	Cu	Ni	Pt
Resistivity (20°C, μΩ cm)	1.673	6.84	10.6
Density (20°C, g cm^{-3})	8.92	8.9	21.45
Length [a] (cm)	1173	287	185
Mass (mg)	205	50.1	77.9
Heat capacity [b] (mJ K^{-1})	79	22	11
TCR ($10^{-3}K^{-1}$)	4.3	6.81	3.92

(a) a wire of 0.05 mm having a resistance of 100 Ω at 20°C.
(b) values at 25°C.

III. FABRICATION PROCESS FOR THE PROTOTYPE

The ridges of human fingerprint are generally 450-μm wide, so, a 225-μm-pitch sensor (112 dpi) is theoretically enough in

order to get the relevant signal information [14]. We fabricated 200-μm pitch of sensor element array as the first generation prototype of the PI film-based approach, which is enough pitch for the experiment to demonstrate the proposed sensing principle. It is not a problem to fabricate a prototype, which have finer pitch of element array (<100 μm), by means of the presented process technology. The limitation of through-hole size by wet etching can be overcome employing laser technology, with which as small as 5-μm-diameter of uniform through holes can be created on the PI film substrate.

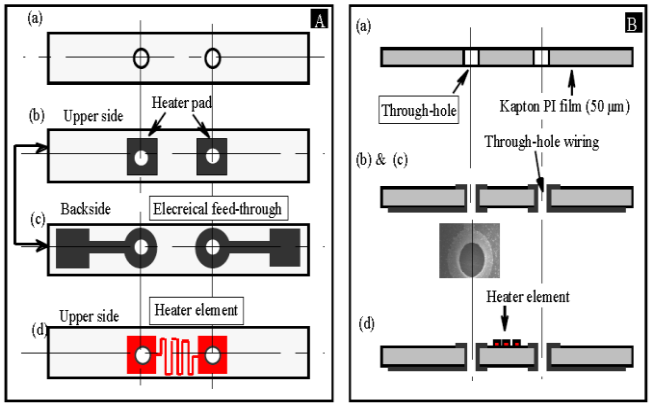

Fig. 6 Fabrication process of micro heater array having interconnected through hole metal film wiring: (A) top views, and (B) cross sectional views.

Figure 6 shows the schematic drawing of the fabrication process: (A) is top views, and (B) is cross-sectional views. The starting material is 50-μm thick Kapton PI film. In Fig. 6-(a), by PI film wet etching technology, Φ60-μm of through-holes is created. Then, PI film chemical pretreatment is performed in a strong alkaline solution TPE3000 at the condition of 70°C/7sec, in order to promote adhesion of thin metal film to the PI film. As shown in Fig. 6-(b) & (c), by photolithography and electroless copper-plating technology, the through-hole interconnection is realized between the upper side heater pad and backside electrical feed-through. A 1-μm thick heater pad and electrical feed-through as well as the through hole wiring are created by electroless plating technology at the same process. In Fig. 6-(d), by photolithography, platinum sputtering and lift-off patterning, one-dimensionally arrayed heater elements are created on the upper side surface of PI film substrate. 20-nm-thick titanium film is sputtered firstly as the adhesion tie layer, followed by 200-nm-thick platinum layer which acts as the sensing elements. Radio frequency (RF) magnetron sputtering equipment RSC-3ERD is used in our fabrication process. The whole fabrication process is simple, cost effective and realized at a low temperature range (<130°C) on the non-silicon and flexible substrate. The fabricated sensor wafer is flexible enough to be attached to non-planar curved surface as show in Fig. 4.

Figure 7 shows the Optical microscopy picture of the fabricated prototype structure. The proposed sensor structure and the fabrication technology will be useful for a variety of extended applications of 2- or 3-D distribution sensors with high resolution, and high sensitivity. For example, the applications of micro temperature distribution sensors and micro flow distributions, in addition to the micro fingerprint sensors. The low temperature process will enable the device in a state of higher reliability.

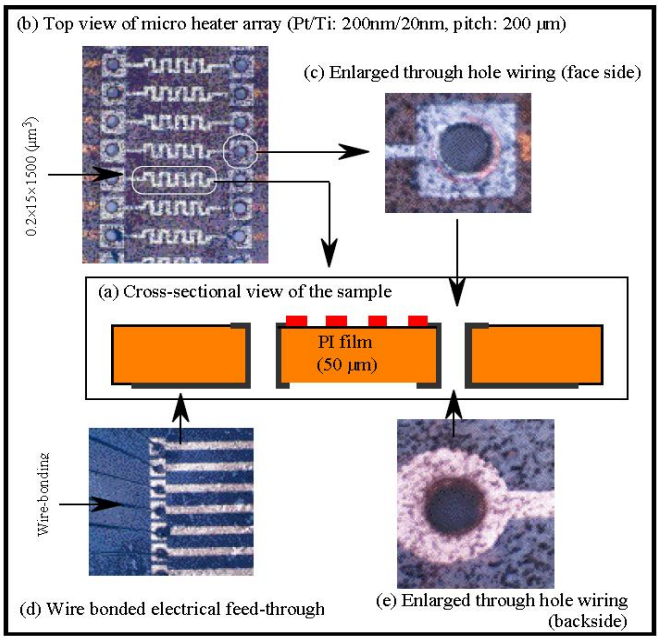

Fig. 7 Fabricated prototype structure of polymer-based arrayed micro thermal sensor: (a) cross-sectional view of the sample; (b) top view of the one-dimensionally arrayed micro heater elements; (c) top view of the enlarged through hole wiring; (d) bottom view of the feed-through with wire bond; (e) bottom view of the enlarged through-hole wiring (Wiring: ϕ30-μm of aluminum wire).

IV. Experimental Results and Evaluation

A. TCR of the sensing elements

If the temperature coefficient is independent of temperature, the relationship between the resistance and the temperature (*R*-*T*) of the material can be written as

$$R(T) = R(T_0)(1+\alpha(T-T_0)) \qquad (1)$$

Where, T_0 is the ambient temperature. TCR was obtained by measuring the sensing element's resistance variation in a precisely controlled resistive oven by slowly changing its temperature. The temperature was checked from the display of the oven, and confirmed by measuring with a thermocouple thermometer at the same time. The detection circuit is shown in Fig. 8. A constant direct current (I_S = 1mA) was used to drive the circuit. The DC power I_S drives a precise measuring current through the conducting lead wire L1 and L4. The conducting lead wire L2 and L3 measure the voltage drop across the heater element. Figure 9 shows the temperature dependence of the heater resistance. From the Resistance-Temperature curve, it is easy to understand that the TCR is very little dependence on the temperature. The regression line is obtained using least square error fitting. The TCR value of the heater element (Pt/Ti film) derived from the fitted line is $2.9\times10^{-3}K^{-1}$. I-V curve under the stable state is useful to characterize the thermal properties of a micro-heater. Because micro-heater is a pure resistor device, the resistance and power can be derived from the I-V curve. The temperature of the micro-heater can be calculated from the TCR value and the measured resistance variations of the heater.

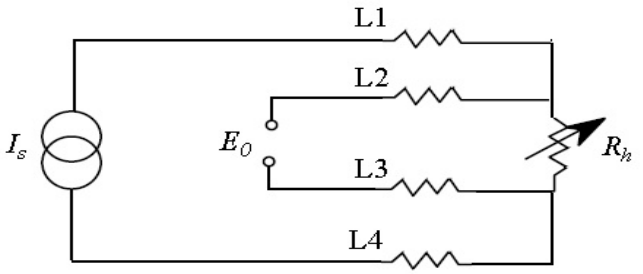

Fig. 8 Detection circuit for measuring TCR of the heater elements. 1mA of constant direct current I_s is applied as the driven current. I_s drives a precise measuring current through the conducting lead wires L1 and L4. The voltage drop E_0 across the heater element R_h is measured through the conducting lead wires L2 and L3.

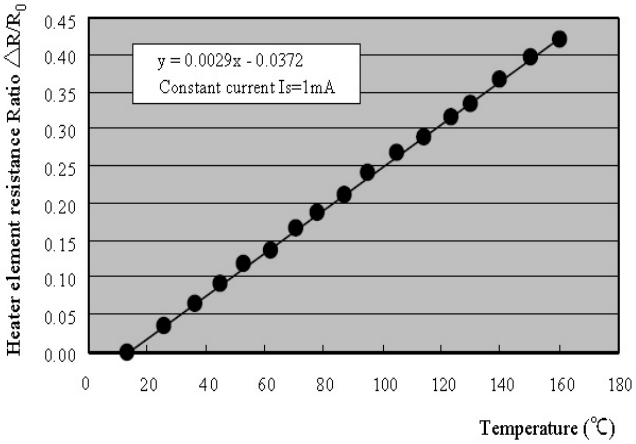

Fig. 9 Electrical resistance-ratio of the heater element vs. applied temperature (Calculated TCR: 0.0029 K^{-1}).

B. Temperature-current relationship

The relationship between the temperature and the input current for the micro heater element was obtained by calculation from the I-V curve and the TCR value as well as the measured resistance variations under the stable states. Figure 10 shows the calculated results. A noticeable discrepancy from the straight line can be observed because of the relatively high positive TCR of the heater elements and the good thermal isolation between the heater elements and the substrate. At a 25mA of input, the heater element is heated from the room temperature to 150°C.

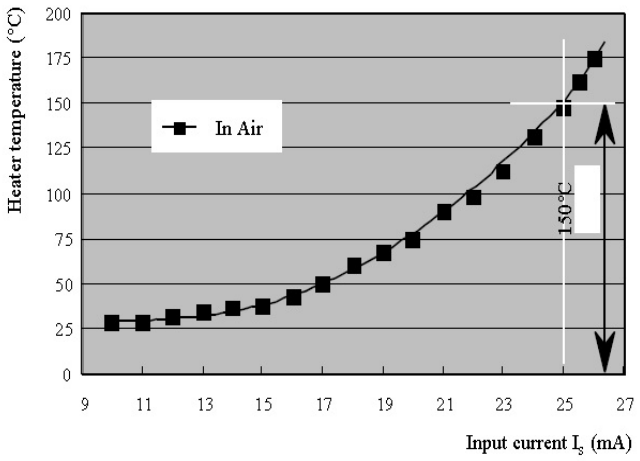

Fig. 10 The dependence of micro-heater temperature to applied current in air ambient.

C. Heat transmission ratios at the device structure

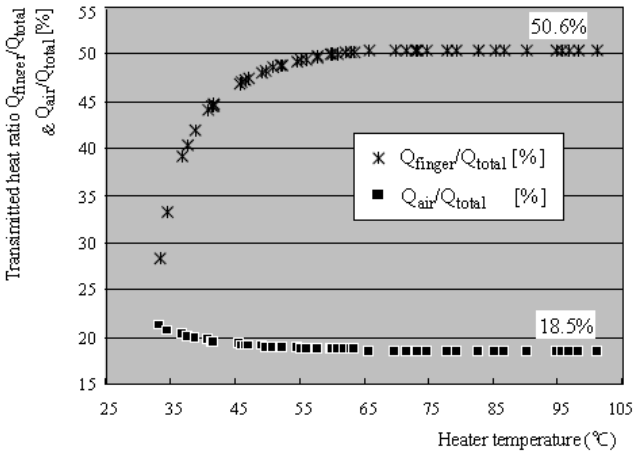

Fig. 11 Transmitted heat ratio vs. the temperature rise. Two situations are compared: (1) human fingertip is in contact with the sensor surface; (2) sensor is in the air ambient and no fingertip is in contact with the sensor surface. In the condition of (1), the heat transmission ratio from the heater element to the fingertip is shown using mark✱. In the condition of (2), the heat transmission ratio from the heater element to the ambient air is shown using mark■ .

If the heat transmission by radiation is ignored due to the low heater temperature («300°C), the heat generated by the input current on the heater element will be transmitted by the following two ways: one is to the substrate (including wiring) by conduction and the other one is to the surrounding air by convection. The consumed power at the heater element can be calculated from the I-V curve. Below, describes such a situation, i.e., the heater element is in the air ambient, in vacuum and in contact with human fingertip, respectively. In vacuum, the heat from the heater element will be completely transferred to the sensor substrate, while in the air ambient, it will be transferred to the sensor substrate and air. Therefore, when the sensor is in air, we can separate the amount of heat transferred to the substrate and to the air by the following equations:

$$Q_{sub} / Q_{air} = P_{vacuum} / (P_{air} - P_{vacuum}) = K \quad (2)$$

$$Q_{total} = Q_{sub} + Q_{air} = KQ_{air} + Q_{air} = Q_{air} (K + 1) \quad (3)$$

$$Q_{air} / Q_{total} = 1 / (K + 1) \quad (4)$$

$$Q_{sub} / Q_{total} = 1 - Q_{air} / Q_{total} = K (K + 1) \quad (5)$$

Where, P_{vacuum} and P_{air} can be calculated from the I-V curve, and Q_{sub} shows the heat transferred from the heater to the substrate; Q_{air} shows the heat transferred from the heater to the air; Q_{total} shows the amount of heat generated in the heater when the heater is in the air; P_{vacuum} shows the consumed power on the heater element in the state of vacuum; P_{air} shows the consumed power on the heater element in the state of air ambient in order to get the same heater temperature as that of in the vacuum.

With the same way, when a human fingertip is contacting to the sensor surface,

$$Q_{sub} / Q_{finger} = P_{vacuum} / (P_{finger} - P_{vacuum}) = K' \quad (6)$$

$$Q_{total} = Q_{sub} + Q_{finger} = Q_{finger} (K' + 1) \quad (7)$$

$$Q_{finger} / Q_{total} = 1 / (K' + 1) \quad (8)$$

$$Q_{sub} / Q_{total} = 1 - Q_{finger} / Q_{total} = K' / (K' + 1) \quad (9)$$

Where, Q_{sub} shows the heat transferred from the heater to the substrate; Q_{finger} shows the heat transferred from the heater to the human fingertip; Q_{total} shows the amount of heat generated in the heater in the condition where the heater is in contacting with human fingertip; P_{vacuum} shows the consumed power on the heater element in the state of vacuum; P_{finger} shows the consumed power on the heater element in the condition where the human fingertip is contacting to the heater surface and the heater temperature is same as that of in the vacuum; P_{vacuum} and P_{finger} can also be calculated from the I-V curve.

Figure 11 shows the transmitted heat ratio versus heater temperature. Converting was made from the experimental results of TCR and I-V curve. Two different situations were compared in Fig. 11: (1) a fingertip is in contact with the sensor surface; (2) nothing but air is around the sensor surface. When the sensor was exposed in the air ambient without fingertip contacting, 18.5% of the total heat Q_{total} generated in the heater was transferred to the air and the left of 81.5% went to the substrate. However, when a human fingertip was in contact with the sensor surface, 50.6% of the heat was transferred to the human fingertip and the left of 49.4% was transferred to the substrate. When the human fingertip is in contact with the sensor surface, heat transmission balance is significantly changed comparing to the state of non-finger-contacting. Consequently, the finger print patterns can be detected by comparing the resistance change of each heater elements.

D. Thermal response

The thermal response of the heater element, which driven by a square-wave pulse voltage, was measured. Figure 12 shows the transient temperature response when the heater element is driven by 5.4V/1kHz of the input pulse voltage. The heater element's temperature can be calculated from the TCR value and the measured resistance variations of the heater. Very fast temperature response was realized on the heater element due to its excellent thermal isolation to the substrate, and the small thermal capacity of the heater element. Experimental results show that, in about 0.1-μs of time, the heater element's temperature was risen from the room temperature of 24°C to the near 300°C. Even such a high level of temperature, the heater element did not hurt the fingertip skin due to the small heat capacity of the heater element. When the skin is already in contact with the device surface before the current is input, the heater element never shows such a temperature rise. The maximum temperature of the heater can also be adjusted by the input power according to the situation of applications.

Features of the short response time is a great advantage in the design of high-resolution applications, enable to realize whole response in *ms*-orders of time by small power consumption, when the layout of element array is a big amount for example 300×300.

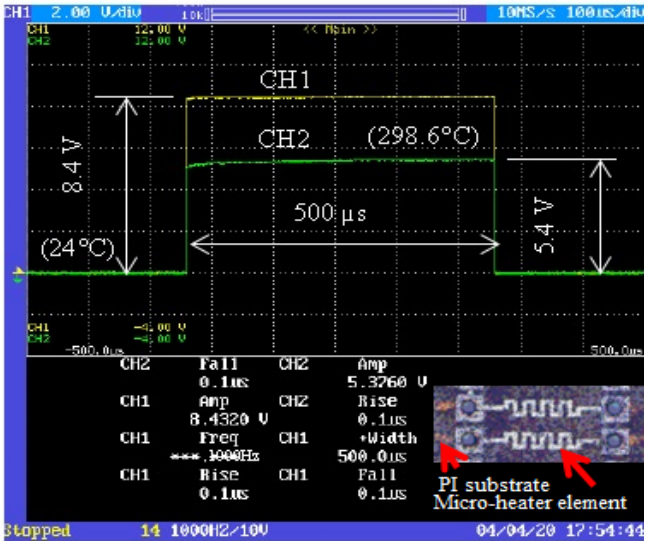

Fig. 12 Transient temperature response of the heater element driven by 5.4V/1kHz of square-wave pulse. Picture was taken from the digital oscilloscopic output wave during experiments.

V. SUMMARY

Depending on the simulation results the authors have proposed a new thermal sensor structure having improved thermal properties which has the features of flexibility and 3-D though-hole wiring. Experiment was performed using the fabricated polymer-based prototype and demonstrated the sensing principle considering the most severe application situation of fingerprint captures as the example. In the proposed sensor structure, a thin (50-μm thick) flexible Kapton PI film was used as the sensor substrate and a sputtered 200-nm thick platinum film was used as the sensing material and patterned to the heater elements by lift-off technique. Sensing elements and electrical feed-through were arranged on the different sides of the substrate and interconnected by through-hole wiring by means of the PI film wet etching and electroless copper plating technology.

The following conclusions can be summarized:

1. The whole fabrication process is simple and realized at a low temperature (<130°C), on the low-cost and flexible non-silicon substrate.
2. Developed sensor device was flexible enough and could be attached to a non-planer curved surface easily, enable a wider range of technical and application extension.
3. By means of the metal film through-hole wiring, the sensing elements and the wiring (feed-through) could be arranged at the different sides of the substrate, which enabling the management of the sensing elements much easier in 2-D array systems and make the sensing reliable.
4. TCR of the Pt heater elements was 2.9×10^{-3} K^{-1} with good linearity.
5. Extremely fast temperature response and sensitivity was realized by this sensor, due to the effective thermal isolation and the small thermal capacity. When a 5.4-V/1kHz of the pulse voltage was applied to the heater element, the temperature of the heater could be risen from room the temperature to the near 300°C in about 0.1-μs of the time. It is a great advantage in the design of high-resolution applications, enable to realize whole

response in *ms* order of time, even if the layout of element array is 300×300.

6. Through the simulation analysis in our prior work, it was become clear that in the thermal sensor design, the most sensitive parameters for the sensor properties are thermal conductivity of the substrate and the sensing elements as well as their thermal capacity besides the thermal isolation between the sensing elements and the substrate of the device. These design points are demonstrated by our prior work of silicon-based approach as well as the polymer-based approach in this work experimentally.

REFERENCES

[1] Kurt Gieck, Technische Formelsammlung, Jan. 1987, translated by Ohda Hiroshi.
[2] "MEMS Material Database: Measurements", http://mems.isi.edu/mems/materials/measurements.cgi
[3] Catalogue, Kapton Polyimide film, Du Pont-Toray Co., ltd., Japan.
[4] Catalogue, Upilex Polyimide film, Ube Industries, Ltd., Japan.
[5] http://www.kapton-dupont.com/
[6] http://www.ube-ind.co.jp/
[7] Doseok Kim, Y.R. Shen: "Study of wet treatment of polyimide by sum-frequency vibrational spectroscopy", Appl. Phys. Lett., 74, pp. 3314-3316, (1999).
[8] Ji-song Han (Hirofumi Miki), Zhi-yong Tan, K Sato and M Shikida: "Three-dimesional interconnect technology on a flexible polyimide film", J. Micromech. Microeng. 14 (2004) 38-48.
[9] Marta M.D. Ramos: "Theoretical study of metal-polyimide interfacial properties", Vacuum 64 (2002), pp. 255-260.
[10] Hirofumi Miki, S. Tsuchitani: "Structural design points in arrayed micro thermal sensors (I) ~ silicon-based approach ~ ", International Journal of Engineering and Technical Research (IJETR), 7 (2) 2017, 36-44.
[11] J. W. Gardner, "Microsensors, Principles and Applications", John Wiley & Sons, Chichester, 1994.
[12] G. C. M. Meier and A. W. van Herwaarden, "Thermal sensors", Institute of Physics Publishing Bristol and Philadelphia, 1994.
[13] T. Ricolfi, J. Scholz, "Sensors, A comprehensive survey, Volume 4, Thermal Sensors", VCH, 1990.
[14] Jean-Francois Mainguet, Marc pegulu and John B. Harris, Fingerprint
[15] recognition based on silicon chips, Future Generation Computer Systems 16 (2000) 403-415